Chinese Chemical Letters 28 (2017) 2290–2294

Contents lists available at ScienceDirect

Chinese Chemical Letters

journal homepage: www.elsevier.com/locate/cclet

Communication

Analysis of graphene-like activated carbon derived from rice straw for application in supercapacitor

Kevin Monthiego Horax, Shujuan Bao*, Minqiang Wang, Yanan Li

Institute for Clean Energy & Advanced Materials, Faculty of Materials & Energy, Southwest University, Chongqing 400715, China

ARTICLE INFO

Article history:
Received 11 September 2017
Received in revised form 24 October 2017
Accepted 6 November 2017
Available online 8 November 2017

Keywords:
Rice straw
Graphene-like
Activated carbon
Supercapacitor
2D-layer

ABSTRACT

Activated carbons with large surface area, abundant microporosity and low cost are the most commonly used electrode materials for energy storage devices. However, activated carbons are conventionally made from fossil precursors, such as coal and petroleum, which are limited resources and easily aggregate large block in high temperature carbonization processes. In this novel work, we examined the use of rice straw as a potential alternative carbon source precursor for the production of graphene-like active carbon. A very slack activated carbon with ultra-thin two-dimensional (2D) layer structure was prepared by our proposed approach in this work, which includes a pre-treatment process and potassium hydroxide activation at high temperatures. The obtained active carbon derived from rice straw exhibited a capacitance of 255 F/g at 0.5 A/g, excellent rate capability, and long cycling capability (98% after 10,000 cycles).

Current environmental crises have stimulated tremendous research efforts to develop advanced technologies and exploit environmentally-friendly energy sources and energy storage devices. Due to fast charging-discharging feature [1], high power density [1,2], and long cycle life [1–4] research on supercapacitors has attracted extensive interest.

Generally, various nano-structured carbons, such as activated carbon [5], graphene [6], carbon nanotubes [7], carbon nanofiber [8], aerogel carbon [9], and porous carbon [10], have been commonly studied in energy conversion and storage devices due to their immense surface area, good electrical conductivity, excellent physicochemical stability, and high degree of surface reactivity. Among these materials, activated carbons (ACs) exhibit the largest surface area, abundant micro-porosity, and lowest production cost [11,12]; thus, they are the most used electrode material for energy storage. However, ACs are conventionally made from fossil precursors, such as coal and petroleum, which are limited resources and easily aggregate large block in high-temperature carbonization processes [13]. ACs formed in a dense and compact large bulk seriously limit their application in energy conversion and storage technologies due to their poor core accessibility to electrolyte ions. Therefore, scientists have begun searching for alternative by-product feedstocks that are environmentally friendly, have unlimited presence, and have easy and inexpensive production processes to replace fossil precursors [14,15]. On the other hand, two-dimensional (2D) carbon materials, such as graphene, have a low-dimension structure that can shorten ion-diffusion lengths and be an effective electron transport in electrochemical reaction processes. Hence, an extensive effort has been devoted to perform controllable exfoliation of graphite to prepare 2D layer-structured active carbon materials.

Rice straw has become the largest agricultural waste in the world, especially in Asia where rice is the staple food for most of the Asian population. Therefore, rice straw has the potential to be utilized for value addition rather than burned or naturally self-decomposed on paddy fields [16]. In rice straw biomass, celluloses, hemicelluloses, and lignin bind together *via* hydrogen bonds to form microfibrils of several nanometers in diameter and several millimeters in length, which are the fundamental structural units in rice straw cell walls [17,18]. In this work, we prepared a novel graphene-like active carbon using rice straw as the carbon source. This approach includes two processes, namely pre-treatment and potassium hydroxide activation. During the pre-treatment process, hydrogen bonds within cellulose, hemicellulose, and lignin were interrupted, and decomposed into polysaccharide polymers and even down to sugar monomers [19,20] where hydrogen peroxide acted as an oxidative agent to oxidize the cell wall of rice straw [21]. Sulfuric acid helped to shorten the reaction [22,23], while

* Corresponding author.
E-mail address: baoshj@swu.edu.cn (S. Bao).

https://doi.org/10.1016/j.cclet.2017.11.004

potassium hydroxide was used as an activation agent that aided the formation of rich pores on the carbon materials [24]. Potassium hydroxide activation also prompted the formation of slack layer structure during the sintering process and accelerated the thermal exfoliation of carbon to form a graphene-like product. The effects of pre-treatment and potassium hydroxide activation on the structure and morphology of prepared active carbon were investigated in detail in this work. Herein, we propose a possible forming process for activated carbon using rice straw as a precursor, which is displayed in Fig. 1. In addition, the electrochemical properties of the obtained products as electrodes for supercapacitors were also estimated.

The microstructures and morphologies of the activated carbons prepared using different processes were first observed by scanning electron microscope (SEM). As seen in Fig. 2A, the precursor obtained by pre-treatment exhibits a rough and slack surface. After further carbonization at high temperature, the product (RSPT, Fig. 2B) became dense and compacted, while RS-A sample (activated by potassium hydroxide without pre-treatment process) had a smooth surface but was still extremely compacted (Fig. 2C). It is interesting to note that RSPT-A had a very slack and thin layered structure with a rough and wrinkled surface (Figs. 2D and E), which is far different than RSPT and RS-A. The detailed morphology and microstructure of RSPT-A were further observed by transmission electron microscope (TEM). It is clear that RSPT-A was very slack and consisted of ultra-thin two-dimensional (2D)-layer structure, which is similar to graphene reported in previous literature [25,26]. From this result, it can be concluded that both potassium hydroxide activation and the pre-treatment process influenced the structure and morphology to become thin and small as well as to form the platform similar to graphene. The thickness of RSPT-A was further observed by atomic force microscope (AFM). As shown in Fig. S1 (Supporting information), it was around 1.6 nm which is near to some reported graphene (~1 nm) [27].

Nitrogen adsorption-desorption experiments were further performed to investigate the effects of pre-treatment and potassium hydroxide activation on the specific surface area and porosity structure of the activated carbons. As shown in Fig. 3A, the three samples have different characteristic curves, where RSPT displayed a type IV characterization curve [28] specified by a wider and vertical plateau with a hysteresis loop, suggesting that RSPT is a mesoporous material. The curve of RS-A exhibited type I characterization [28] due to the presence of a sharp bend in the beginning followed by a horizontal plateau without a hysteresis loop. This means that RS-A was dominated by micropores in the absence of mesopority. Unlike the two aforementioned curves, the RSPT-A curve showed a combination characteristic between type I and type IV curves, where a vertical plateau occurred with a sharp elbow in the presence of a hysteresis loop. This characteristic indicates that RSPT-A was dominated by both micropores and mesopores. The specific surface areas of RSPT, RS-A, and RSPT-A were 34.97, 214.13, and 317.6 m^2/g, respectively. Combined with the SEM observation, it can be concluded that the pre-treatment process aided to form a slack and rough surface, which facilitated KOH to fully immerse into the corresponding precursor. After the subsequent potassium hydroxide activation at a high temperature, rich pores formed and the carbons were exfoliated to a large extent.

The X-ray diffraction (XRD) patterns of all prepared carbons are shown in Fig. 4A, which are highly similar to the active carbon reported in previous study [29]. A broad peak at $2\theta = 23.6^\circ$ corresponds to (002) crystal plane diffraction peak of graphite, suggesting the presence of amorphous carbon [29]. A low peak at $2\theta = 43.6^\circ$ represents the convolution of (1 0) hk bi-dimensional lines, where the presence of hk lines caused the turbostatic stacking of hexagonal layer, as reported in the previous work. This result confirms the formation of a disordered carbon [30]. The graphitic structures of the samples were further analyzed by Raman spectra, as shown in Fig. 4B. The two characterization peaks located at around 1320 cm^{-1} (D-band) and 1580 cm^{-1} (G-band), respectively correspond to k-point phonons for disordered graphite and to 2D-graphite, which is related to the vibration of sp^2-hybridized atoms in a two-dimensional hexagonal lattice [31]. The intensity relation between the D-band and G-band (I_D/I_G) is commonly used to identify the crystallization degree of carbon materials. The values of I_D/I_G from RSPT, RS-A and RSPT-A were determined to be 1.39, 1.15 and 1.1, respectively. Considering these differences, it can be concluded that the pre-treatment process followed by potassium hydroxide activation significantly enhanced the graphitization degree of the activated carbon with RSPT-A having the highest degree.

X-ray photoelectron spectroscopy (XPS) was used to investigate the chemical composition of RSPT-A. The content of carbon, oxygen, nitrogen and sulphur in RSPT-A was 78.69%, 20.56%, 0.58% and 0.17%, respectively. The five split peaks from the high resolution C 1s spectrum shown in Fig. 4C correspond to sp^2-bonded carbon (284.36 eV), sp^3-bonded carbon (285.46 eV) [32], C=O (288.41 eV), and satellite peaks π—π^* (292.7 eV and 295.48 eV) [33,34]. Pyridinic nitrogen (397.8 eV), pyrrolic nitrogen (399.4 eV), and quaternary nitrogen (402.3 eV) were observed in the N 1s spectrum (Fig. 4D) [35]. Quaternary nitrogen is a nitrogen that bonds to three C atoms and is located in the middle or valley position of the graphene layer, pyridinic nitrogen bonds to two C atoms of a six-member ring at the side of the graphene layer, and pyrrolic nitrogen is part of a five-member ring that bonds to the carbonyl group on the carbon atoms of the ring [13]. As reported in literatures, the presence of pyrrolic and pyridinic nitrogen, could enhance the pseudocapacitive of actived carbon whereas quaternary nitrogen is effective to improve the conductivity of electrode materials and contributes to the cycling performance of supercapacitors [35–38]. As shown in Fig. 4E, the high resolution XPS spectra of S 2p show three peaks at 163.4, 165.3, and 168.1 eV,

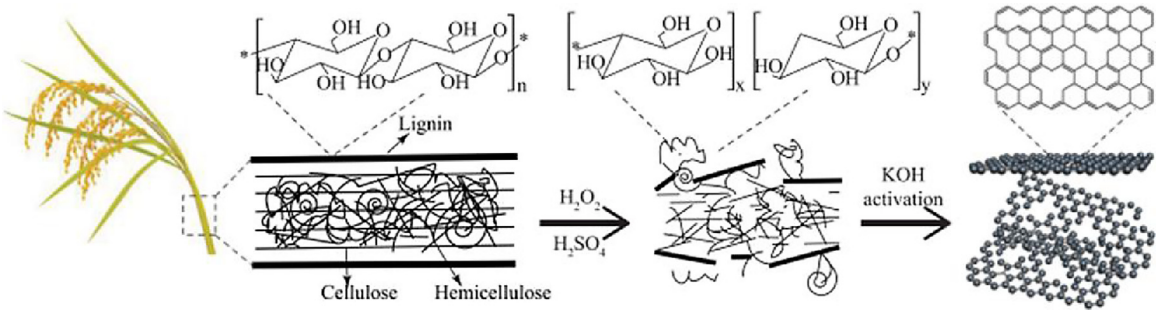

Fig. 1. Scheme of the formation process of graphene-like activated carbon derived from rice straw.

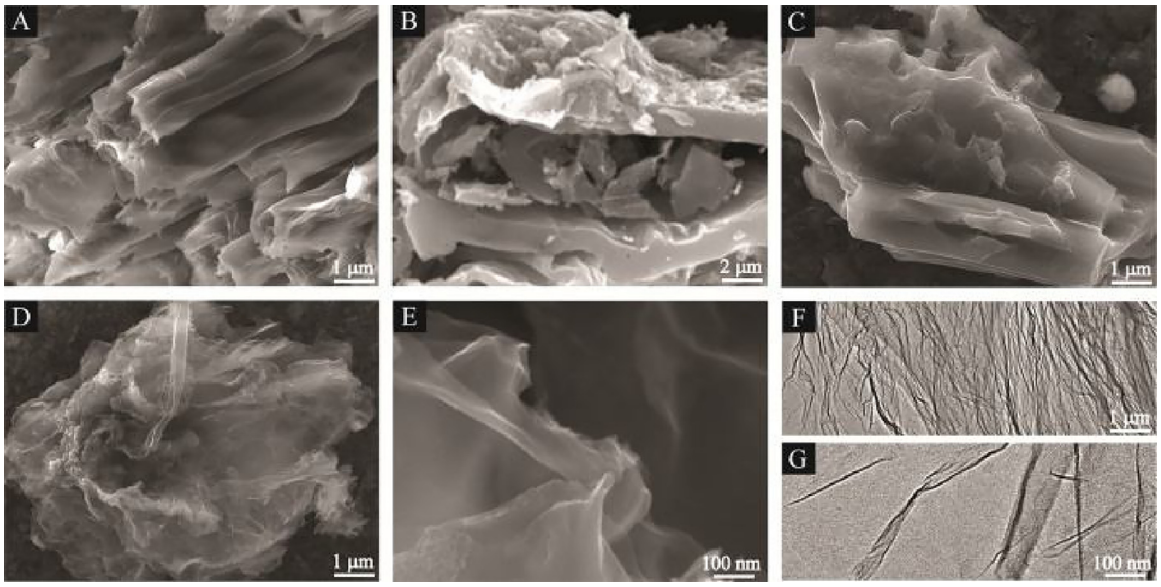

Fig. 2. SEM images of (A) rice straw after pre-treatment, (B) RSPT, (C) RS-A, and (D and E) RSPT-A; and (F and G) TEM images of RSPT-A.

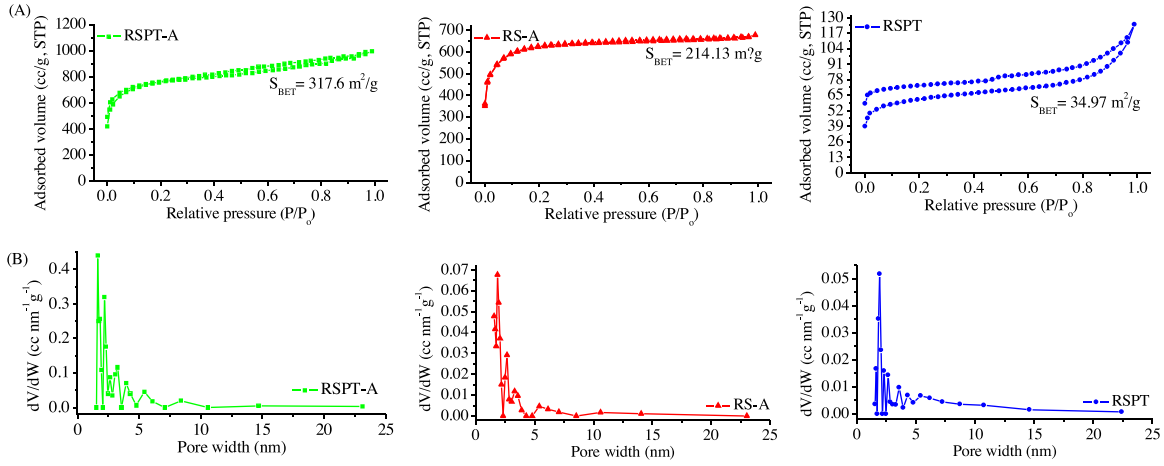

Fig. 3. (A) N_2 adsorption-desorption isotherms, and (B) pore size distributions of all samples.

which are related to $2p_{3/2}$, $2p_{3/2}$, and oxidized sulfur groups [38], respectively. The introduction of sulphur atoms in active carbons could provide a polarized surface as well as reversible *pseudo*-site and thus resulting in superior performance. Fig. 4F shows an O 1s spectrum that reveals the presence of oxygen-containing functional groups in the sample. The first peak at a binding energy of 531.61 eV could be identified as a carbonyl group (C=O) and/or quinone, whereas the second peak at a binding energy of 533.06 eV reveals a hydroxyl group (C—OH) [36]. The presence of carbonyl, hydroxyl groups and sulphur relative groups also could effectively improve the hydrophilicity of materials, and facilitate the movement of electrolyte ions within the material [1,36], further enhance the electrochemical performance of materials.

Based on the characteristics of the three carbon samples, the activated carbon derived from rice straw presents a big potential for energy storage, particularly for the application of supercapacitors. To further understand the electrochemical performance of RSPT, RS-A, and RSPT-A, a cyclic voltammetry (CV) study was performed using a three-electrode system, where 3 mol/L aqueous potassium hydroxide served as the electrolyte solution. Fig. 5A shows the CV curves of all samples at a scan rate of 100 mV/s. All curves display a rectangular-like shape with a hump at the low potential region, which indicates a combination effect between the electric double-layer capacitance (EDLC) and the *pseudo*-capacitance caused by the existence of heteroatoms of active nitrogen, sulfide, and/or oxygen [35–38]. Based on the CV study, RSPT-A exhibited a larger and wider area than others, meaning this sample had the highest specific capacitance. This high capacitance was promoted by the structure and morphology of the activated carbon in RSPT-A, where the very thin and rich porous structure allowed for faster electrolyte ion transport and a shorter inter-electron diffusion distance [31].

The performance capacity of all samples was evaluated by a galvanostatic charge-discharge (GCD) experiment at a scan rate of 0.5 A/g with the potential window set to the same parameters as the CV analysis. The specific capacitances from electrode materials were calculated based on the discharge GCD curves using Eq. (1).

$$C_{sp} = (I \times \triangle t)/(m \times \triangle v) \quad (1)$$

As shown in Fig. 5B, all curves display a symmetrical shape and linearity, indicating the characteristics of an ideal capacitor. The specific capacitance values of RSPT, RS-A and RSPT-A were 67, 186,

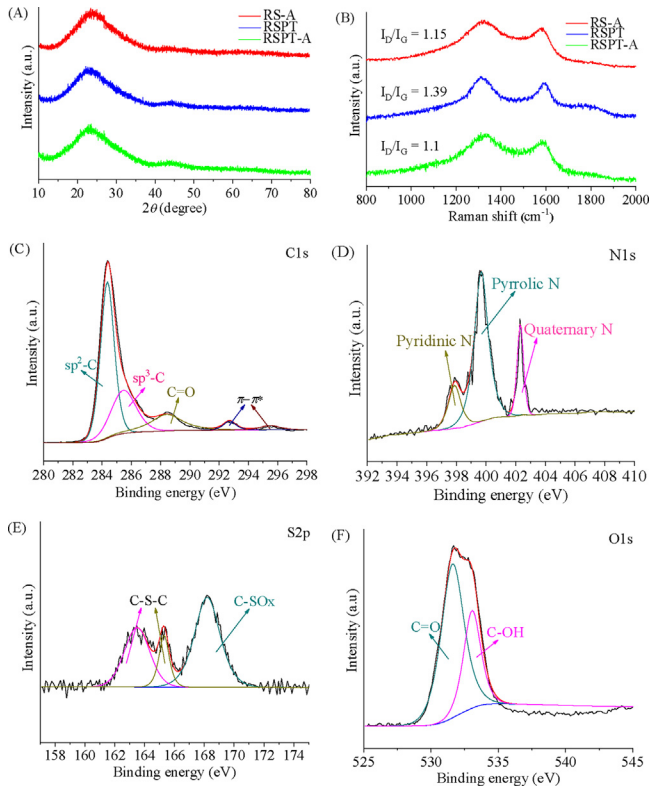

Fig. 4. (A) XRD pattern and (B) Raman spectra of RS-A, RSPT and RSPT-A. (C) C 1s XPS spectra, (D) N 1s XPS spectra, (E) S 2p XPS spectra, and (F) O 1s XPS spectra of RSPT-A.

and 255 F/g, respectively. Although a higher current density means a lower specific capacitance because ions can only partially penetrate into micropores [14,39], RSPT-A still maintained a good specific capacitance of 205 F/g at a current density of 10 A/g due to the presence of mesopores on its surface which facilitated rapid electron transfer and a high degree of graphitization, further enhancing the conductivity of the electrode.

Considering all aforementioned results, it is suggested that RSPT-A is an excellent electrode candidate for supercapacitors due to its structure and morphology that is similar to graphene, large specific surface area, and excellent ion diffusion rate. To verify the capability of RSPT-A in such applications, CV and GCD experiments were tested at various scan rates, and a long-term cyclic experiment was analyzed to determine its capacitance retention. As shown in Fig. 6A, all CV curves of RSPT-A analyzed at scan rates of 5, 10, 20, 50, and 100 mV/s display a rectangular-like shape. In addition, the resulting curves from GCD experiments at different current densities (0.5, 1, 2, 5, and 10 A/g) (Fig. 6B) show perfect and symmetric lines that confirm good rate reversibility of adsorption-desorption on the electrode surface. Fig. 6C displays various patterns between the capacitance retention and cycle number for RSPT-A at a current density of 2 A/g. This result suggests a good stability cycle along the double-layer electrochemical process, while the capacitance retention of RSPT-A reached 98% after 10,000 charge-discharge cycles.

In summary, RSPT-A had the highest specific capacitance and proved to be the best stability cycle electrode material. The activated carbon exhibited an ultra-thin layer that was rich in both micro- and mesopores, which were attributable to the pre-treatment process and potassium hydroxide activation. Moreover, the presence of rich surface active heteroatoms of nitrogen and/or oxygen-containing functional groups also improved the hydrophilic capability of the activated carbon, further enhancing the ion diffusion rate in electrolyte solution.

A graphene-like activated carbon was produced from rice straw through a hydrogen peroxide-sulfuric acid pre-treatment process followed by potassium hydroxide activation and analyzed for its electrode application in supercapacitors. In the pre-treatment process, hydrogen peroxide is a strong and efficient oxidant, which could decompose organic compounds and increase the oxygenated functional group of the obtained materials. But only using hydrogen peroxide, the reaction is time consuming. In this work, sulfuric acid could further enhance the reaction rate and shorten

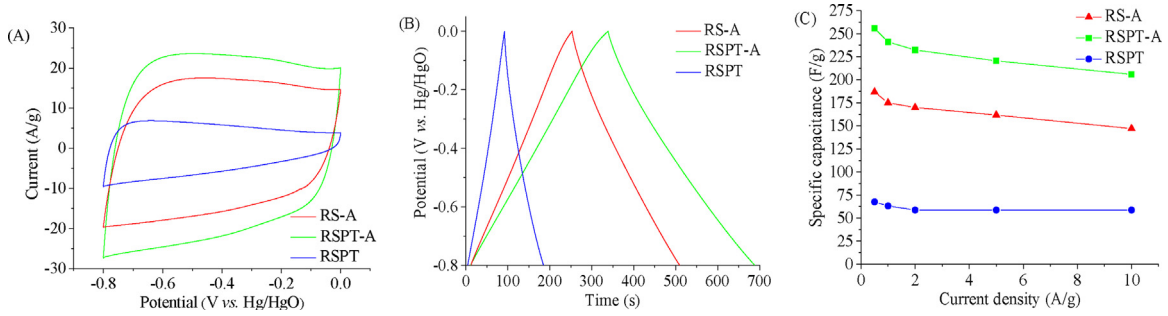

Fig. 5. (A) CV curves (100 mV/s), (B) GCD curves (0.5 A/g), and (C) specific capacitance *vs.* current density of RS-A, RSPT and RSPT-A.

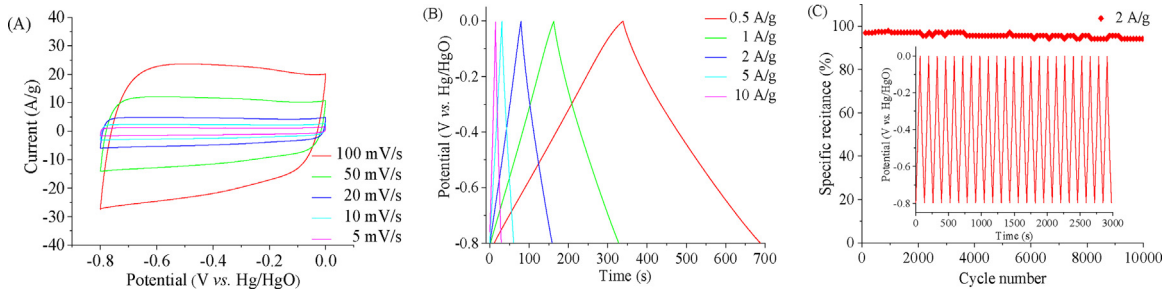

Fig. 6. (A) CV curves, (B) GCD curves, and (C) cycle performance of RSPT-A.

the reaction time of the oxidation process. The pre-treatment process plays an important role in forming graphene-like active carbon. Hydrogen bonds within cellulose, hemicellulose and lignin could be interrupted during pre-treatment process, and then the structure of rice straw will be decomposed by potassium hydroxide easily, which helps accelerate the thermal exfoliation of the carbon to form a graphene-like product. Following activation with potassium hydroxide at 750 °C, the material exhibited a thin graphene-like layer that was rich in both micro-and mesopores. The results from the electrochemical characteristic study in 3 mol/L KOH showed that its specific capacitance reached 255 F/g at a scan rate of 0.5 A/g and a high capacity retention (98%) after 10,000 charge-discharge cycles. In conclusion, based on its electrochemical performance, the superconductor prepared with RSPT-A appears to be promising for application as an energy storage device.

Acknowledgments

This research was financially supported by the Fundamental Research Funds for the Central Universities (Nos. XDJK2017D003, XDJK2017B055), the Program for Excellent Talents in Chongqing (No. 102060-20600218), the Program for Innovation Team Building at Institutions of Higher Education in Chongqing (No. CXTDX201601011), and the Chinese Government Scholarship (No. 2016AUN032).

References

[1] Y. Li, J. Xu, H. Xia, et al., Adv. Funct. Mater. 27 (2017) 1606728.
[2] N. Jabeen, Q.Y. Xia, H. Xia, et al., ACS Appl. Mater. Interfaces 8 (2016) 33732–33740.
[3] L.L. Zhang, X.S. Zhao, Chem. Soc. Rev. 38 (2009) 2520–2531.
[4] J. Yan, Q. Wang, T. Wei, Z. Fan, Adv. Energy Mater. 4 (2014) 1300816.
[5] J. Gamby, P.L. Taberna, P. Simon, et al., J. Power Sources 101 (2001) 109–116.
[6] Y.W. Zhu, S. Murali, M.D. Stoller, et al., Science 332 (2011) 1537–1541.
[7] Y. Zhao, W.L. Wu, J.X. Li, et al., Adv. Mater. 26 (2014) 5113–5118.
[8] L.H. Bao, J.F. Zang, X.D. Li, Nano Lett. 11 (2011) 1215–1220.
[9] W.C. Li, G. Reichenauer, J. Fricke, Carbon 40 (2002) 2955–2959.
[10] C.W. Huang, Y.T. Wu, C.C. Hu, et al., J. Power Sources 172 (2007) 460–467.
[11] H.L. Wang, Z.W. Xu, A. Kohandehghan, et al., ACS Nano 7 (2013) 5131–5141.
[12] J.C. Wang, S. Kaskel, J. Mater. Chem. 22 (2012) 2371–23725.
[13] K. Wang, N. Zhao, S.W. Lei, et al., Electrochem. Acta 166 (2015) 1–11.
[14] A.G. Pandolfo, A.F. Hollenkamp, J. Power Sources 157 (2006) 11–27.
[15] M.M. Titirici, R.J. White, C. Falco, et al., Energy Environ. Sci. 5 (2012) 6796–6822.
[16] E.Y. Vlasenko, H. Ding, J.M. Labavith, et al., Bioresour. Technol. 59 (1997) 109–119.
[17] X.L. Chen, J. Yu, Z.B. Zhang, C.H. Lu, Carbohydr. Polym. 85 (2011) 245–250.
[18] D. She, X.N. Nie, F. Xu, et al., Cellulose Chem. Technol. 46 (2012) 207–219.
[19] Y. Sun, J.Y. Cheng, Bioresour. Technol. 83 (2002) 1–11.
[20] D. Akmal, M.R. Marjoni, F. Ismed, J. Chem. Pharm. 7 (2015) 570–575.
[21] J. Akhsay, B. Rajasekhar, M.P. Srinivasan, Chem. Eng. J. 273 (2015) 622–629.
[22] S.H. Zeronian, M.K. Inglesby, Cellulose 2 (1995) 265–272.
[23] B.G. Petri, R.J. Watts, A.L. Teel, et al., Fundamentals of ISCO using hydrogen peroxide, in: R.L. Siegrist (Ed.), In situ Chemical Oxidation for Groundwater Remediation, Springer science + Business media, LLC, 2011, pp. 33–88.
[24] Y.P. Guo, S.F. Yang, K.F. Yu, et al., Mater. Chem. Phys. 74 (2002) 320–323.
[25] B. Xu, S.F. Yue, Z.Y. Sui, et al., Energy Environ. Sci. 4 (2011) 2826–2830.
[26] C.L. Tan, X.H. Cao, X.J. Wu, et al., Chem. Rev. 117 (2017) 6225–6331.
[27] Y.X. Yao, L.L. Ren, S.T. Gao, et al., J. Mater. Sci. Technol. 33 (2017) 815–820.
[28] L.M. Anovitz, D.R. Cole, Mineral. Geochem. 80 (2015) 61–164.
[29] G.Q. Zhang, S.T. Zhang, J. Solid State Electrochem. 13 (2009) 887–893.
[30] M. Inagaki, New Carbons: Control of Structure and Functions, 1st. ed., Elsevier Science, Oxford, 2000.
[31] L. Sun, C.G. Tian, M.T. Li, et al., J. Mater. Chem. 1 (2013) 6462–6470.
[32] I.K. Moon, J.H. Lee, R.S. Ruoff, et al., Nat. Commun. 1 (2010) 73.
[33] H. Zhu, X.L. Wang, X.X. Liu, et al., Adv. Mater. 24 (2012) 6524–6529.
[34] L. Hao, X.L. Li, L.J. Zhi, Adv. Mater. 25 (2013) 3899–3904.
[35] L.F. Chen, X.D. Zhang, H.W. Liang, et al., ACS Nano 6 (2012) 7092–7102.
[36] D. Hulicova-Jurcakova, M. Seredych, G.Q. Lu, et al., Adv. Funct. Mater. 19 (2009) 438–447.
[37] X.J. Wei, Y.B. Li, S.Y. Gao, J. Mater. Chem. A 5 (2017) 181–188.
[38] J. Liang, Y. Jiao, M. Jaroniec, et al., Angew. Chem. Int. Ed. 51 (2012) 11496–11500.
[39] W. Xing, C.C. Huang, S.P. Zhuo, et al., Carbon 47 (2009) 1715–1722.